Strongly correlated metal interfaces in the Gutzwiller approximation

Giovanni Borghi,[1] Michele Fabrizio,[1,2] and Erio Tosatti[1,2]
[1]*International School for Advanced Studies (SISSA), and CRS DEMOCRITOS, CNR-INFM, Via Beirut 2-4, I-34151 Trieste, Italy*
[2]*The Abdus Salam International Centre for Theoretical Physics (ICTP), P.O. Box 586, I-34151 Trieste, Italy*
(Received 4 November 2009; revised manuscript received 3 February 2010; published 23 March 2010)

We study the effect of spatial inhomogeneity on the physics of a strongly correlated electron system exhibiting a metallic phase and a Mott insulating phase, represented by the simple Hubbard model. In three dimensions, we consider various geometries, including vacuum-metal-vacuum, a junction between a weakly and a strongly correlated metal, and finally the double junctions metal-Mott insulator-metal and metal-strongly correlated metal-metal. We apply the self-consistent Gutzwiller technique recently developed in our group, whose approximate nature is compensated by an extreme flexibility, ability to treat very large systems, and physical transparency. The main general result is a clear characterization of the position-dependent metallic quasiparticle spectral weight. Its behavior at interfaces reveals the ubiquitous presence of exponential decays and crossovers with decay lengths of clear physical significance. The decay length of the metallic strength in a weakly-strongly correlated metal interface is due to poor screening in the strongly correlated side. That from a metal into a Mott insulator is due to tunneling. In both cases, the decay length is a bulk property and diverges with a critical exponent ($\sim 1/2$ in the present approximation, mean field in character) as the (continuous, paramagnetic) Mott transition is approached.

DOI: 10.1103/PhysRevB.81.115134 PACS number(s): 73.20.−r, 71.10.Fd, 71.30.+h

I. INTRODUCTION

Metallic electron wave-function delocalization in a lattice of atoms or molecules is caused by the lowering of electron kinetic energy and by the simultaneous improvement of electron-ion Coulomb attraction. By abandoning the ion cores and turning delocalized, an electron can in fact feel the potential of more than one nucleus. However, coherent electron motion is opposed by the mutual electron-electron Coulomb repulsion, which is higher when electrons move, due to their higher chance of colliding when visiting the same site. When the first two terms prevail, the system is a conventional band insulator or metal, depending whether the Fermi level falls in a band gap or across one or more bands. When the electron-electron repulsion prevails instead the electrons localize on their atomic or molecular sites leading to a so-called Mott insulator.[1] Despite that conceptual simplicity, properties of Mott insulators and especially of strongly correlated metals in the proximity of a Mott metal-insulator transition as a function of increasing correlations remain quite difficult to capture both theoretically and experimentally. Theoretically, the reason is that the Mott transition is a collective phenomenon, which escapes single-particle or mean-field theories such as Hartree-Fock or density-functional-theory within the local-density approximation (LDA). Experimentally, additional complications such as magnetism, lattice distortions, etc., often conspire to mask the real nature of the Mott localization phenomenon.

Important insights into this problem have been gained in the last two decades especially thanks to dynamical mean-field theory (DMFT).[2] DMFT predicts that, as the electron-electron repulsion—usually parametrized by a short-range Hubbard repulsion U—increases, the ordinary band metal evolves first to a *strongly correlated metal* well before the Mott transition. In the strongly correlated metal the electron spectral function undergoes a profound change, exhibiting well-formed Mott-Hubbard side-bands coexisting with delocalized quasiparticles, the latter narrowly centered in energy near the Fermi level. Only successively upon increasing repulsion do the quasiparticles disappear as the Mott transition takes place at $U=U_{\mathrm{crit}}$. This intriguing prediction—simultaneous metallic and insulating features, exhibited on well-separated energy scales—has stimulated a considerable experimental effort to reveal coexisting quasiparticles and Mott-Hubbard bands in strongly correlated metals,[3–12] especially in the paradigmatic system V_2O_3. This is the compound where a Mott transition has been first discovered[13] and theoretically studied.[14,15] At ambient temperature and pressure V_2O_3 is a correlated metal. It undergoes a first-order Mott transition at $\sim T_N \simeq 155$ K to an antiferromagnetic insulator accompanied by a monoclinic distortion of the high-temperature corundum structure.[16] The paramagnetic high-temperature metal can moreover be turned into a paramagnetic Mott insulator upon substituting V with bulkier Cr, $(V_{1-x}Cr_x)_2O_3$. For $0.005<x<0.017$ a first-order line separates the high-temperature metal from the paramagnetic Mott insulator, which terminates with a critical point at $T \simeq 400$ K and $x \simeq 0.005$.

Near the metal-insulator transition of $(V_{1-x}Cr_x)_2O_3$, the strongly correlated metal must of course possess well-defined quasiparticles at the Fermi energy. Surprisingly, early photoemission experiments[17–20] failed to reveal the sharp quasiparticle peak predicted by DMFT at E_F. The electronic spectrum appeared instead dominated by the lower Mott-Hubbard band with barely a hint of metallic weight at the Fermi energy. It was recognized only later that photoemission in strongly correlated metals is highly surface sensitive.[3,4,6,7,11,12,21] By increasing the photon frequency, which corresponds to more energetic excited photoelectrons, i.e., longer escape lengths, a prominent quasiparticle peak coexisting with incoherent Mott-Hubbard bands was eventually observed in V_2O_3.[5,10,22] Quasiparticle suppression in surface-sensitive probes was attributed[22] to surface-modified

Hamiltonian parameters, the reduced atomic coordination pushing the surface closer to the Mott transition than the underlying bulk. This conclusion, although not unreasonable, raised however a more fundamental question. A metal does not possess any intrinsic long-distance electronic length scale other than the Fermi wavelength. Thus an imperfection such as a surface can only induce a power-law-decaying disturbance such as that associated with Friedel's oscillations. Since one does not expect Luttinger's theorem to break down, these oscillations should be controlled by the same Fermi wavelength as in the absence of interaction, irrespectively of the proximity of the Mott transition. On the other hand, a strongly correlated metal does possess an intrinsic energy scale, the parametric distance of the Hamiltonian from the Mott transition, and that could be associated with a length scale. The surface as a perturbation may alter the quasiparticle properties within a depth corresponding to that characteristic length. We expect this length to be a bulk property, the longer the closer the Mott transition, unlike the Fermi wavelength that remains constant. In this respect, it is not *a priori* clear whether the recovery of bulk-quasiparticle spectral properties with increasing depth should be power law, compatible with the common view of a metal as an inherently critical state of matter, or exponential, as one would expect by regarding the Mott transition as any other critical phenomena where power laws emerge only at criticality.

Besides the interface with vacuum, which is relevant to spectroscopy, other types of interface involving correlated materials are attracting increasing interest. In 2004, Ohtomo and Hwang[23] discovered that the interface between two insulating oxides, $LaAlO_3$ and $SrTiO_3$, is a high-mobility two-dimensional conductor that even shows superconductivity.[24] This discovery stimulated experimental and theoretical studies on oxides heterostructures.[25] On the theory side, some activity focused either on the characterization of the electronic structure of these interfaces by *ab initio* LDA calculations, see, e.g., Ref. 26, as well as on DMFT analyses of simple models[27–35] and on combined LDA-DMFT calculations[36] aimed at understanding interface-correlation effects poorly described within straight LDA. The DMFT approaches adopted in the literature to describe this kind of situations were *ad hoc* extensions of the single-site DMFT (Ref. 2) to inhomogeneous systems.[27,28] In the specific example of a layered structure, the electron self-energy was assumed to depend, besides the frequency, also upon the layer index. In this scheme the self-energy is calculated by solving an auxiliary impurity model for each layer in which the conducting bath depends self-consistently on the fully interacting impurity Green's functions not only of that given layer but also of the nearby ones. This additional complication with respect to conventional DMFT weighs on the numerical calculation, which is thus limited to few tens of layers. Although this is adequate for the interface between two insulators, such as that studied by Ohtomo and Hwang,[23] it is generally insufficient in other cases, such as the surface effects in the interior of a correlated metal,[37] or any other interface involving at least one metal.

Recently, we proposed an alternative theoretical approach to interface problems,[38] based on the extension of the Gutzwiller wave function and approximation[39,40] to inhomogeneous situations. The method, although a further approximation beyond DMFT, hence, in principle, less accurate, is much more agile, and can treat without effort hundreds of layers. Thus it can be used as a complementary tool to extrapolate DMFT results to large sizes, otherwise inaccessible by straight DMFT.

In this work, we shall extend the analysis of Ref. 38 for the vacuum/correlated-metal interface to other model interfaces that might be relevant for experiments: the junction between two different correlated metals and the tunneling between two metallic leads through a strongly correlated, possibly Mott insulating, region. Although both cases were in fact previously studied by DMFT,[31,34,35] the results were interpreted in contrasting ways. While Helmes *et al.*[34] concluded that the Mott insulator is impenetrable to the electrons coming from the metallic leads, Zenia *et al.*[35] drew the opposite conclusion that a conducting channel always open up inside the insulator at sufficiently low temperature. The present study, which is certainly less accurate than DMFT but can deal with much larger sizes, will also serve to clarify this issue. In particular, the large sizes allow us to address the asymptotic behavior and to identify the magnitude and interface role of the critical length associated with the bulk Mott transition.

The paper is organized as follows. In Sec. II we introduce the model Hamiltonian, which is a Hubbard model with layer-dependent parameters, and a Gutzwiller variational scheme adapted for such an inhomogeneous situation. We then study in Sec. III three different slab geometries: (a) strongly correlated metal-vacuum interface; (b) junction between two differently correlated metals; and (c) a Mott insulator or a strongly correlated metal sandwiched between two weakly correlated metals. In the two former cases we find that the perturbation induced by the surface inside the bulk of the correlated metal decays exponentially at long distances. The length scale ξ that controls this decay is a bulk property that depends in our simplified model only on $U_{\mathrm{crit}} - U$ and diverges on approaching the Mott transition such as $\xi \sim (U_{\mathrm{crit}} - U)^{-\nu}$, with a mean-fieldlike exponent $\nu \simeq 0.5$. Results of the last case (c) offer additional interest. Both when the central region, of width d, is a strongly correlated metal, $U_{\mathrm{center}} < U_{\mathrm{crit}}$ and when it is a Mott insulator, $U_{\mathrm{center}} > U_{\mathrm{crit}}$, the additional metallic weight brought by the two metal leads is found to decay exponentially into the central region over a length ξ. Like in cases (a) and (b) above, ξ is only controlled by the distance from Mott criticality, i.e.,

$$\xi \sim |U_{\mathrm{crit}} - U_{\mathrm{center}}|^{-0.5},$$

which therefore appears naturally as a correlation length that is finite on both sides of the transition. However, while the quasiparticle weight saturates to a finite constant determined by $U_{\mathrm{center}} < U_{\mathrm{crit}}$ and independent of d when the central region is a strongly correlated metal, in the opposite case of a Mott insulator the quasiparticle weight reaches in the slab center a value exponentially small in d. Interestingly, right at criticality, $U_{\mathrm{center}} = U_{\mathrm{crit}}$, the decay turns power law in d. Finally, Sec. IV is devoted to concluding remarks.

II. MODEL AND METHOD

In order to address the generic interface features of a strongly correlated metal, we consider the simplest Hamiltonian exhibiting a Mott transition, namely, the Hubbard model

$$H = -\sum_{\langle \mathbf{R}\mathbf{R}'\rangle\sigma} t_{\mathbf{R}\mathbf{R}'}(c^{\dagger}_{\mathbf{R}\sigma}c_{\mathbf{R}'\sigma} + \text{H.c.}) + \sum_{\mathbf{R}} \epsilon_{\mathbf{R}} n_{\mathbf{R}} + U_{\mathbf{R}} n_{\mathbf{R}\uparrow} n_{\mathbf{R}\downarrow}, \tag{1}$$

where $\langle \mathbf{R}\mathbf{R}'\rangle$ denotes nearest-neighbor sites, $c^{\dagger}_{\mathbf{R}\sigma}$ and $c_{\mathbf{R}\sigma}$ create and annihilate, respectively, an electron at site $\mathbf{R}$ with spin σ, and finally $n_{\mathbf{R}\sigma}=c^{\dagger}_{\mathbf{R}\sigma}c_{\mathbf{R}\sigma}$ and $n_{\mathbf{R}}=n_{\mathbf{R}\uparrow}+n_{\mathbf{R}\downarrow}$. In our inhomogeneous system, all Hamiltonian parameters are allowed to be site dependent. For interfaces, we shall assume an N-layer slab geometry where all parameters are constant within each layer, identified by a layer coordinate $z=1,\ldots,N$ but generally different from layer to layer. For instance, the hopping between nearest-neighbor sites $\mathbf{R}$ and $\mathbf{R}'$ within layer z depends only on z, i.e., $t_{\mathbf{R}\mathbf{R}'}=t(z)$ while if $\mathbf{R}$ and $\mathbf{R}'$ belong to nearby layers, e.g., z and $z\pm 1$, then $t_{\mathbf{R}\mathbf{R}'}=t(z,z\pm 1)=t(z\pm 1,z)$.

We study the Hubbard Hamiltonian (1) in the nonmagnetic (sometimes called paramagnetic) sector by means of a Gutzwiller-type variational wave function

$$|\Psi\rangle = \prod_{\mathbf{R}} \mathcal{P}_{\mathbf{R}} |\Psi_0\rangle, \tag{2}$$

where $|\Psi_0\rangle$ is a paramagnetic Slater determinant. Because of our choice of layer-dependent parameters, the operator $\mathcal{P}_{\mathbf{R}}$ has the general expression

$$\mathcal{P}_{\mathbf{R}} = \sum_{n=0}^{2} \lambda_n(z) |n,\mathbf{R}\rangle\langle n,\mathbf{R}|, \tag{3}$$

where $|n,\mathbf{R}\rangle\langle n,\mathbf{R}|$ is the projector at site $\mathbf{R}=(x,y,z)$, (x and y are intralayer coordinates), onto configurations with n electrons (note that $|1,\mathbf{R}\rangle\langle 1,\mathbf{R}| \equiv \Sigma_{\sigma} c^{\dagger}_{\mathbf{R}\sigma}|0,\mathbf{R}\rangle\langle 0,\mathbf{R}|c_{\mathbf{R}\sigma}$), and $\lambda_n(z)$ are layer-dependent variational parameters. We calculate quantum averages on $|\Psi\rangle$ using the so-called Gutzwiller approximation,[39,40] (for details see, e.g., Ref. 41 whose notations we use hereafter) and require that

$$\langle \Psi_0 | \mathcal{P}^2_{\mathbf{R}} | \Psi_0 \rangle = 1, \tag{4}$$

$$\langle \Psi_0 | \mathcal{P}^2_{\mathbf{R}} n_{\mathbf{R}\sigma} | \Psi_0 \rangle = \langle \Psi_0 | n_{\mathbf{R}\sigma} | \Psi_0 \rangle \equiv \frac{n(z)}{2}. \tag{5}$$

Explicitly, these two conditions imply that

$$1 = \left[1 - \frac{n(z)}{2}\right]^2 \lambda_0(z)^2 + n(z)\left[1 - \frac{n(z)}{2}\right]\lambda_1(z)^2 + \frac{n(z)^2}{4}\lambda_2(z)^2, \tag{6}$$

$$n(z) = n(z)\left[1 - \frac{n(z)}{2}\right]\lambda_1(z)^2 + 2\frac{n(z)^2}{4}\lambda_2(z)^2. \tag{7}$$

We note that $n(z)$ is fixed once the uncorrelated variational wave function $|\Psi_0\rangle$ is given. In reality, we find more convenient to treat $n(z)$ as an additional variational parameter and constrain $|\Psi_0\rangle$ to span all paramagnetic Slater determinants that have a fixed local charge density $n(z)$. The average value of Eq. (1) within the Gutzwiller approximation is accordingly given by[41,42]

$$E = \frac{\langle \Psi | H | \Psi \rangle}{\langle \Psi | \Psi \rangle} \simeq \sum_{\mathbf{R}} U_{\mathbf{R}} \frac{n(z)^2}{4}\lambda_2(z)^2 + \epsilon_{\mathbf{R}} n(z) - \sum_{\langle \mathbf{R}\mathbf{R}'\rangle\sigma} t_{\mathbf{R}\mathbf{R}'} R(z) R(z') \langle \Psi_0 | c^{\dagger}_{\mathbf{R}\sigma} c_{\mathbf{R}'\sigma} + \text{H.c.} | \Psi_0 \rangle, \tag{8}$$

where

$$R(z) = \left[1 - \frac{n(z)}{2}\right]\lambda_0(z)\lambda_1(z) + \frac{n(z)}{2}\lambda_1(z)\lambda_2(z) \tag{9}$$

plays the role of a wave-function-renormalization factor, whose square can be regarded as the actual layer-dependent quasiparticle weight, $Z(z)=R^2(z)$. Because of Eqs. (6), (7), and (9), one can express

$$\lambda_n(z) = \lambda_n[R(z), n(z)]$$

as a functional of the two variational functions $R(z)$ and $n(z)$. Furthermore, the single-particle wave functions that define the Slater determinant $|\Psi_0\rangle$ can be chosen, for a slab geometry, to have the general expression

$$\phi_{\epsilon\mathbf{k}_{\parallel}}(\mathbf{R}) = \sqrt{\frac{1}{A}} e^{i\mathbf{k}_{\parallel}\cdot\mathbf{R}} \phi_{\epsilon\mathbf{k}_{\parallel}}(z),$$

where A is the number of sites per layer and $\mathbf{k}_{\parallel}$ the momentum in the x-y plane. The minimum of E, Eq. (8), can then be obtained by searching for saddle points with respect to the variational parameters $R(z)$, $n(z)$ and $\phi_{\epsilon\mathbf{k}_{\parallel}}(z)$, the latter subject to the constraint

$$\frac{2}{A} \sum^{occupied} |\phi_{\epsilon\mathbf{k}_{\parallel}}(z)|^2 = n(z)$$

the sum running over all occupied states in the Slater determinant.

Considerable simplifications arise if we further assume a bipartite lattice with a Hamiltonian (1) invariant under the particle-hole transformation

$$c_{\mathbf{R}\sigma} \to \sigma(-1)^R c^{\dagger}_{\mathbf{R}-\sigma},$$

where $(-1)^R$ is $+1$ on one sublattice and -1 on the other. This symmetry requires $\epsilon_{\mathbf{R}}=0$ in Eq. (1) and implies $n(z)=1$ hence $\lambda_0(z)=\lambda_2(z)$ and $\lambda_1(z)^2=2-\lambda_0(z)^2$. In this case the saddle point is simply obtained by solving the coupled equations

$$\epsilon\phi_{\epsilon\mathbf{k}_{\parallel}}(z) = R(z)^2 \epsilon_{\mathbf{k}_{\parallel}}(z)\phi_{\epsilon\mathbf{k}_{\parallel}}(z) - R(z)\sum_{p=\pm 1} t(z,z+p) \times R(z+pa)\phi_{\epsilon\mathbf{k}_{\parallel}}(z+pa), \tag{10}$$

$$R(z) = \frac{4\sqrt{1-R(z)^2}}{U(z)A} \sum_{\epsilon \mathbf{k}_\parallel}^{occupied} \Big[-2R(z)\epsilon_{\mathbf{k}_\parallel}(z)\phi_{\epsilon\mathbf{k}_\parallel}(z)^2 + \phi_{\epsilon\mathbf{k}_\parallel}(z) \sum_{p=\pm a} t(z,z+p)R(z+pa)\phi_{\epsilon\mathbf{k}_\parallel}(z+pa) \Big], \tag{11}$$

where $\epsilon_{\mathbf{k}_\parallel}(z) = -2t(z)(\cos k_x a + \cos k_y a)$. The first equation has the form of a Schrödinger equation which the single-particle wave functions $\phi_{\epsilon\mathbf{k}_\parallel}(z)$ must satisfy, the quasiparticle hopping now depending parametrically on $R(z)$. The second equation has been intentionally cast in the form of a map $R_{j+1}(z) = F[R_j(z), R_j(z+a), R_j(z-a)]$ whose fixed point we have verified to coincide with the actual solution of Eq. (11) in the parameter region of interest.

In spite of the various assumptions above, solving this saddle-point problem remains, in principle, a formidable task. Fortunately, Eqs. (10) and (11) can in fact be solved relatively easily, by the following iterative procedure. First solve the Schrödinger equation at fixed $R_j(z)$; next find the new $R_{j+1}(z)$ using the old $R_j(z)$ and the newly determined wave functions $\phi_{\epsilon\mathbf{k}_\parallel}(z)$. With the new $R_{j+1}(z)$, repeat the above steps and iterate until some desired level of convergence is reached. Because of the large number of variational parameters, this iterative scheme is much more efficient than—but fully equivalent to—a direct minimization of E, Eq. (8). Away from particle-hole symmetry, the saddle-point equations get more involved but the solution can be obtained along the same lines.

Before concluding, we recall for future use the Gutzwiller approximation results for the Mott transition at particle-hole symmetry in the homogeneous case, $\epsilon_{\mathbf{R}} = 0$, $t_{\mathbf{R}\mathbf{R}'} = t$, and $U_{\mathbf{R}} = U$, i.e., when the variational parameters $\lambda_n(z)$ are z independent. In this case, the solution of Eqs. (10) and (11) is trivial. The critical values $U = U_{\text{crit}}$ at the Mott transition are $U_{\text{crit}} = 32t/\pi$ (for a linear chain), $U_{\text{crit}} = 128t/\pi^2$ (for a square lattice), and $U_{\text{crit}} = 16t$ (for a cubic lattice). The quasiparticle weight Z in terms of the electron-electron interaction U has the simple expression

$$Z = R^2 = 1 - \frac{U^2}{U_{\text{crit}}^2} \tag{12}$$

linearly vanishing at the Mott transition.[15]

III. INTERFACES IN THE THREE-DIMENSIONAL (3D) HUBBARD MODEL: RESULTS

We use the technique just exposed to study 3D simple cubic Hubbard model interfaces in a slab geometry with in-plane (xy) translational symmetry and layer (z)-dependent Hamiltonian parameters. We assume for simplicity particle-hole symmetry and site-independent hoppings $t_{\mathbf{R}\mathbf{R}'} = t$ throughout so that the only source of inhomogeneity is a layer-dependent $U(z)$. The minimization procedure here amounts to solve the coupled Eqs. (10) and (11) with constant hoppings. Technically, we diagonalize the in-plane k-dependent Hamiltonian (10) at every point of a Monkhorst-Pack k grid.[43] The two-dimensional grid used is 32×32, chosen so as to yield well-converged values not just for the quasiparticle weight (for that a 4×4 grid is sufficient) but also for the hopping-matrix element for the geometries and interaction parameters considered. At every iteration j, we choose the convergence indicator

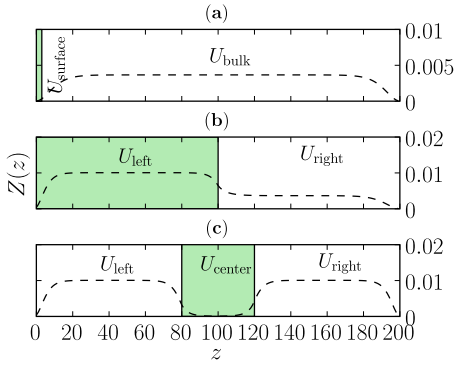

FIG. 1. (Color online) Three different inhomogeneous geometries are studied in this paper: (a) free strongly correlated metal-vacuum interface; (b) junction between metals with different strengths of correlation; and (c) Mott (or strongly correlated metallic) slab sandwiched between metallic leads. For all cases we show the behavior of the quasiparticle weight $Z(z)$ for values of U that are, respectively: (a) $U_{\text{surface}} = 20t$ and $U_{\text{bulk}} = 15.9712t$; (b) $U_{\text{left}} = 15.9198t$ and $U_{\text{right}} = 15.9712t$; and (c) $U_{\text{left}} = U_{\text{right}} = 15.9198t$ and $U_{\text{center}} = 16.0288t$ (which is the case of a Mott central slab).

$$Q_j = \frac{1}{N}\left[\sum_{i=0}^{N} |Z_j(i) - Z_{j-1}(i)| \right] \tag{13}$$

with a threshold of 10^{-6}. This corresponds to a relative energy convergence of less than 10^{-7}. Calculations of the spatial dependence of the hopping-matrix elements[44] are instead performed with a denser k grid of 64×64 k points.

We consider the three different geometries displayed in Fig. 1: (a) *correlated metal-vacuum interface*: a correlated metal ($U_{\text{bulk}} < U_{\text{crit}}$, where $U_{\text{crit}} = 16t$ is the critical value of U at the Mott transition in the cubic lattice) with a stronger correlated surface ($U_{\text{surface}} > U_{\text{crit}}$). (b) *Weakly correlated metal-strongly correlated metal interface*: a junction between a moderately correlated metal ($U_{\text{left}} < U_{\text{crit}}$) and a strongly correlated one ($U_{\text{right}} \lesssim U_{\text{crit}}$). (c) *Metal-Mott insulator-metal double junction*: a Mott insulator $U_{\text{center}} \gtrapprox U_{\text{crit}}$ or a strongly correlated metal $U_{\text{center}} \lesssim U_{\text{crit}}$ sandwiched between two moderately correlated metallic leads $U_{\text{left}} = U_{\text{right}} < U_{\text{crit}}$. The dashed lines in the panels of Fig. 1 show also the quasiparticle weight $Z(z)$ calculated for a $N = 200$ layer slab in the three geometries and for specific values of the Hamiltonian parameters.

We now discuss each case separately. Before that, it is worth introducing some analytical expressions that fit well the numerical results and provide a very transparent physical interpretation. Near criticality, a diverging correlation length emerges that allows to recast Eq. (11) into a differential equation with appropriate boundary conditions set by the interfaces and by the bulk values of the Hamiltonian parameters.[44]

Let us consider for instance a semi-infinite slab consisting of a strongly correlated metal in contact with a different system. In this case the interface determines the boundary value of $R(z)$, $R(z=0)=R_{\rm surf}$ while the bulk Hamiltonian parameters the asymptotic value $R(z\to\infty)=R_{\rm bulk}=\sqrt{Z_{\rm bulk}}$, where

$$R_{\rm bulk}=\sqrt{1-\left(\frac{U_{\rm crit}}{U_{\rm bulk}}\right)^2}, \tag{14}$$

within the Gutzwiller approximation. We find[44] that

$$Z(z)=R^2(z)=\frac{Z_{\rm bulk}\sinh^2\zeta}{(\cosh\zeta\pm\sqrt{1-Z_{\rm bulk}})^2}, \tag{15}$$

where the plus sign applies when $Z_{\rm surf}<Z_{\rm bulk}$ and the minus sign otherwise while

$$\zeta=\sqrt{6Z_{\rm bulk}}(z+z_*)\equiv\frac{z+z_*}{\xi}. \tag{16}$$

The offset z_* is defined through the surface value $Z_{\rm surf}=Z(z=0)$. This solution provides a definition of the correlation length ξ, which, within the Gutzwiller approximation, diverges at criticality like

$$\xi=\frac{1}{\sqrt{6Z_{\rm bulk}}}\simeq 0.289\left(\frac{U_{\rm crit}}{U_{\rm crit}-U_{\rm bulk}}\right)^{1/2} \tag{17}$$

a typical mean-field behavior.

When the slab is a Mott insulator, $U_{\rm bulk}>U_{\rm crit}$, and is in contact with a metallic system, the latter provides a finite quasiparticle weight decaying inside the insulator[44] as

$$Z(z)=4\lambda\frac{\sinh^2\zeta}{(\sinh^2\zeta+\lambda)^2}, \tag{18}$$

where $\lambda=(U_{\rm bulk}-U_{\rm crit})/U_{\rm bulk}$ and

$$\zeta=\sqrt{6\left(\frac{U_{\rm bulk}-U_{\rm crit}}{U_{\rm crit}}\right)}(z+z_*)\equiv\frac{z+z_*}{\xi}. \tag{19}$$

Again, the offset value z_* defines the surface quasiparticle weight through $Z(0)=Z_{\rm surf}$. As before, Eq. (19) defines a proper correlation length ξ of the Mott insulator which, within the Gutzwiller approximation, is

$$\xi\simeq 0.408\left(\frac{U_{\rm crit}}{U_{\rm bulk}-U_{\rm crit}}\right)^{1/2}. \tag{20}$$

In both cases, $U_{\rm bulk}\gtrsim U_{\rm crit}$ and $U_{\rm bulk}\lesssim U_{\rm crit}$, we find[44] that

$$(z+z_*)^2Z(z)=\frac{2}{3}f(\zeta) \tag{21}$$

has a critical behavior with $f(0)=1$ and

$$f(\zeta\to\infty)=4\zeta^2e^{-2\zeta}$$

for insulating bulks while for metallic bulks

$$f(\zeta\to\infty)=\frac{\zeta^2}{4}.$$

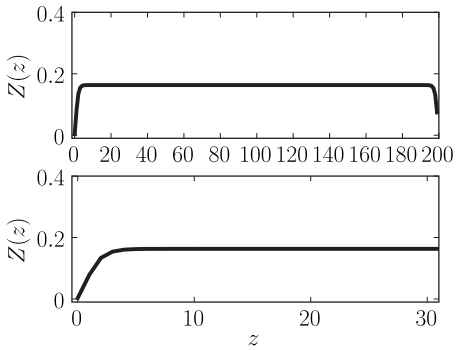

FIG. 2. Spatial dependence of $Z(z)$ for $U_{\rm surf}=20t$ at $z=0$ and $U_{\rm bulk}=14.6642t$, for any $z>0$. The lower panel is the same as the upper one zoomed close to the surface.

A. Geometry (a): correlated metal-vacuum interface

This simple correlated metal-surface case, $U(z>1)=U_{\rm bulk}<U_{\rm crit}$ and $U(z=1)=U_{\rm surface}>U_{\rm crit}$, has been already discussed in detail by Ref. 38, and we just briefly summarize its properties. As shown in Figs. 2 and 3, with values of $U_{\rm surf}=20t$, and $U_{\rm bulk}=9.6t$ and $U_{\rm bulk}=15.97118t$, respectively, there is a so-called *dead layer*[38] at each interface, characterized by a quasiparticle weight Z exponentially decaying from its bulk value, over a typical distance controlled by the bulk correlation length ξ, which diverges on approaching the Mott transition. This loss of surface metallicity is due to the reinforcement of correlations near the surface caused by the reduced coordination and further enhanced on the left surface where $U(z=1)>U_{\rm bulk}$. We note however that, so long as the interior of the slab is metallic, Z at the outer surface atomic layer remains finite, even if very small: there cannot be truly insulating surfaces coexisting with a metallic bulk. In fact, assuming initially such an insulating surface, then simple tunneling from the underlying bulk will bring the metallic quasiparticle weight to a nonzero value, however small. We also find that the analytical expression (15) fits well the numerical results, as shown in Figs. 4 and 5.

Our finding of an exponential recovery, see Eq. (15) for large ζ, of the quasiparticle weight inside the bulk in place of the expected Friedel-type power-law behavior offers a unique opportunity to experimentally access the critical properties of the Mott transition. Photoemission experiments[37] show that the surface depletion of metallic

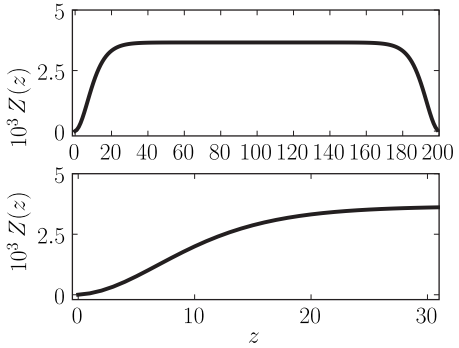

FIG. 3. Same as Fig. 2, for $U_{\rm surf}=20t$ and $U_{\rm bulk}=15.9712t$.

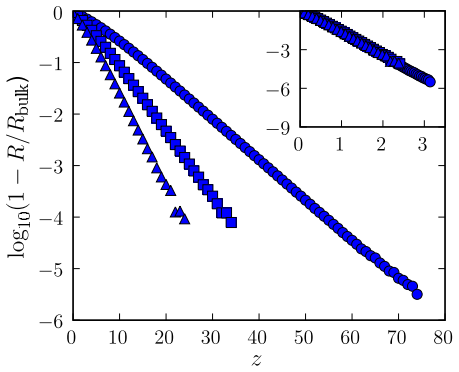

FIG. 4. (Color online) Plot of $\log(1-R/R_{\rm bulk})$ versus z for $U=15.97118t$ (circles), $U=15.9198t$ (squares), and $U=15.84242t$ (triangles). In the inset the same data are plotted with respect to $z(1-U/U_{\rm crit})^{0.5}$.

electron spectral weight in V_2O_3 propagates inside the interior of the sample for an anomalously large depth of many tens of Angstrom beneath the surface, in qualitative agreement with our results, as earlier discussed in Ref. 38.

We end this review by noting that the calculated $Z(z)$ shows an upward curvature near the surface ($z=0$). This differs from earlier results obtained by the so-called linearized DMFT,[28] displaying a linear growth of $Z(z)$ near the surface and very close to criticality. Besides a qualitative agreement with the upward curvature observed in photoemission,[37] (which could be coincidental since the real V_2O_3 is much more complicated than our simple one-band Hubbard model), we do not see strong arguments of principle supporting either approaches. Both Gutzwiller and inhomogeneous linearized DMFT are based on rather uncontrolled approximations. More reliable techniques, such as straight DMFT or quantum Monte Carlo calculations on large size systems, would be needed to clarify this aspect; but this is perhaps not important enough. The important point is that linearized DMFT too appears to lead to a depth of the surface perturbed region that diverges at the Mott transition, just like in our approach.

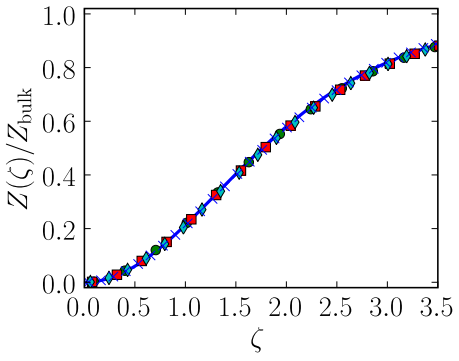

FIG. 5. (Color online) Numerical results for $Z(z)$ in the surface geometry, with $U=15.9872t$ (crosses), $15.9712t$ (diamonds), $15.9487t$ (squares), and $15.9198t$ (circles). The solid curve is a fit with Eq. (15) (with plus sign), with ζ defined as in Eq. (16). The best fit is obtained with a correlation length ξ that, with respect to Eq. (17), has a factor of 3.07 replacing $\sqrt{6}$.

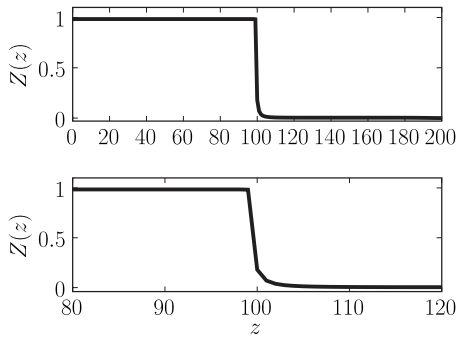

FIG. 6. Spatial dependence of $Z(z)$ for $U_{\rm left}=2t$ and $U_{\rm right}=15.9712t$. The lower panel shows the same data as the upper one but closer to the interface.

B. Geometry (b): weakly correlated metal-strongly correlated metal interface

The junction between a metal and a Mott insulator or a strongly correlated metal was studied recently by Helmes *et al.*,[34] who used the numerical renormalization group as the DMFT impurity solver. With our simpler method we can address a broader class of interfaces, including the general case of a correlated metal-correlated metal junction, with different values of electron-electron interaction in the left ($U_{\rm left}$) and right ($U_{\rm right}$) leads. The system we consider, see Fig. 1(b), is made of two blocks 100 layers each, and the junction center is at $z=N/2$. Figures 6 and 7 show the z dependence of the quasiparticle weight for fixed $U_{\rm right}\simeq U_{\rm crit}$ and two different values of $U_{\rm left}<U_{\rm right}$.

We find that in this case too the numerical data are well described by Eq. (15) with the plus sign on the left side and the minus sign on the right side, see Fig. 8. In other words, the interface affects both sides over a distance that is controlled only by their own bulk correlation lengths, $\xi_{\rm right}$ and $\xi_{\rm left}$ for the right and left slabs, respectively, with $\xi_{\rm right}>\xi_{\rm left}$.

Our results for weak $U_{\rm left}$ and $U_{\rm right}\lesssim U_{\rm crit}$ can be directly compared with those of Helmes *et al.*[34] They proposed that a strongly correlated slab, our right lead with $U_{\rm right}\simeq U_{\rm crit}$, in contact with a weakly interacting metal, our left lead, has a quasiparticle weight $Z(x)$ with, close to criticality, a scaling behavior

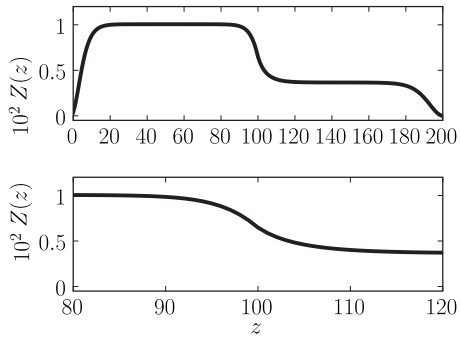

FIG. 7. Same as in Fig. 6, for $U_{\rm left}=15.9198t$ and $U_{\rm right}=15.9712t$.

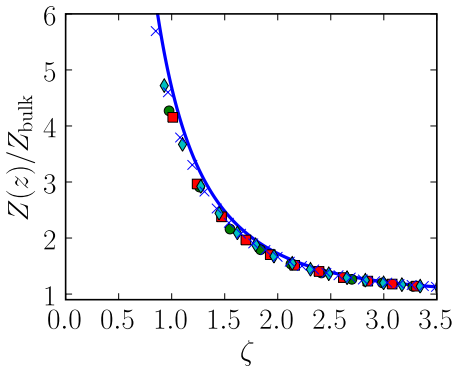

FIG. 8. (Color online) Numerical results for $Z(z)$ in the single-junction geometry with metallic bulk. The position of the interface is the origin for the spatial coordinate, the metal on the left side is very weakly correlated ($U=2t$); the values for U on the right side are the same of Fig. 5. The solid curve is now Eq. (15) with the minus sign. As in Fig. 5, the best fit is obtained by defining ξ with a prefactor 2.87 different from the $\sqrt{6}$ in Eq. (17).

$$x^2 Z(x) \simeq C f\left(x \left| \frac{U - U_{\rm crit}}{U_{\rm crit}} \right|^{1/2}\right), \tag{22}$$

where $f(0)=1$ and x is the distance from the interface, translated in our notation $x=z-N/2$ and $U=U_{\rm right}$. Their prefactor $C\simeq 0.008$ and the asymptotic behavior $f(\zeta\to\infty)=0.15\zeta^2$ of the scaling function were extracted by a DMFT calculation with a 40-layer correlated slab in contact with a 20 layer almost uncorrelated metal.[34]

We show in Fig. 9 the quantity $x^2Z(x)$ extracted by our Gutzwiller technique and plotted versus $x|1-U/U_{\rm crit}|^{1/2}$ for different U's across the Mott transition value. The results are qualitatively similar to those of Ref. 34 but differ in two aspects. First, we find that $f(\zeta)$ defined in Eq. (22) shows a plateau only when

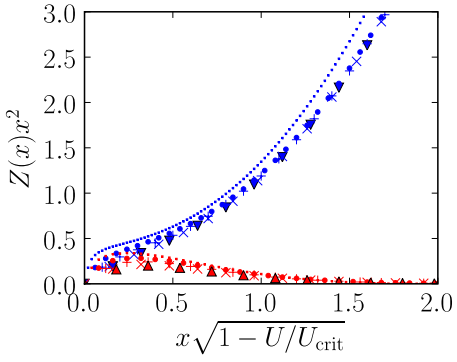

FIG. 9. (Color online) Plot of $Z(x)x^2$ versus the renormalized coordinate $x\sqrt{|1-U/U_{\rm crit}|}$ for $U<U_{\rm crit}$ (upper blue curves: $U=15.7939t$ triangles, $U=15.8424t$ crosses, $U=15.9198t$ pluses, $U=15.9712t$ points, $U=15.9968$ tiny dots), and $U>U_{\rm crit}$ (lower red curves: $U=16.2571t$ triangles, $U=16.2035t$ crosses, $U=16.1148t$ pluses, $U=16.0511t$ points, and $U=16.0128$ tiny dots). This figure can be compared with the inset of Fig. 3 in Ref. 34.

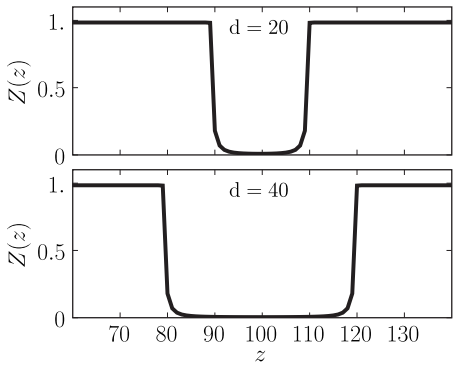

FIG. 10. Spatial dependence of $Z(z)$ for $U_{\rm left}=U_{\rm right}=2t$ and $U_{\rm center}=15.9712t$. The upper panel refers to a central region of $d=20$ layers while the lower panel to $d=40$.

$$z_* \ll x \ll \left| 1 - \frac{U}{U_{\rm crit}} \right|^{-1/2},$$

where the offset value z_* has been defined above. For $x \ll z_*$, $f(\zeta)\sim\zeta^2$ so that $Z(x)$ approaches its surface value at the interface. Our much larger system now makes the crossover between the two different regimes clearly visible. Next, the coefficient $C\simeq 0.08$ found by Helmes *et al.*[34] is almost two orders of magnitude smaller than ours, which is numerically around $\simeq 0.4$, close to the analytical expression $C=2/3$ in Eq. (21). The linearized DMFT approach of Potthoff and Nolting[28] yields a slightly different value[44] $C=9/11\sim 0.82$, of the same order as ours, but again larger than that of Helmes *et al.*[34] Mainly because of the smallness of the prefactor, Helmes *et al.*[34] concluded that the strongly correlated slab with $U\simeq U_{\rm crit}$ hence $Z_{\rm bulk}=Z(x\to\infty)\ll 1$ is very weakly affected by the proximity of the good metal. Our results, as well as linearized DMFT, would not warrant that drastic conclusion. On the other hand, straight DMFT should be more reliable than either linearized DMFT or our Gutzwiller approach so that it is possible that our $Z(x)$ is actually overestimated. It seems therefore worth investigating further this important question with full DMFT on wider slabs.

C. Geometry (c): correlated metal-Mott insulator (strongly correlated metal)-correlated metal double junction

In this section we consider geometry (c) of Fig. 1, in which a strongly correlated slab of d layers is sandwiched between two weakly correlated metal leads, a setup already studied by DMFT.[31,35] In Figs. 10–12 we show the layer dependence of the quasiparticle weight for different values of the interaction parameters, the Hubbard U in the leads, $U_{\rm right}=U_{\rm left}<U_{\rm crit}$, and in the central slab, $U_{\rm center}\gtrless U_{\rm crit}$, and slab thickness d. From these results one can draw the following conclusions: for any finite thickness d, the quasiparticle weight in the central slab never vanishes, as better revealed in Figs. 13 and 14, even for $U_{\rm center}>U_{\rm crit}$, fed as it is by the evanescent metallic quasiparticle strength from the metallic leads. This result agrees perfectly with recent DMFT calculations.[35] For $U_{\rm center}>U_{\rm crit}$, see Fig. 12, the minimum value $Z_{\rm min}$ in the central region decreases when d increases; the behavior of $Z(z)$ across the interface is smoother and

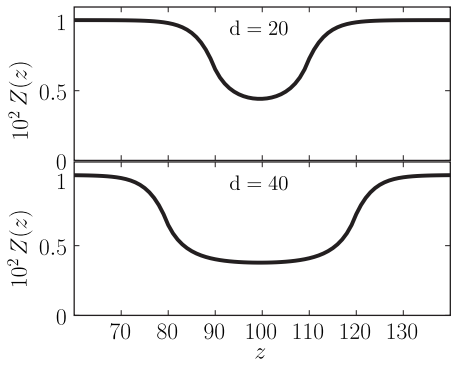

FIG. 11. Same as in Fig. 10, for $U_{\text{left}}=U_{\text{right}}=15.9198t$ and $U_{\text{center}}=15.9712t$.

smoother the closer and closer $U_{\text{right}}=U_{\text{left}}$ are to U_{center}.

Looking in more detail at Figs. 11 and 12 and at the log-scale plots in Figs. 13 and 14, we identify the characteristic differences between a Mott insulating slab and a strongly correlated metallic slab, when sandwiched between metallic leads. In a strongly correlated metallic slab, the central quasiparticle weight ultimately settles to the self-standing value it would have in a homogeneous system with $U=U_{\text{center}}<U_{\text{crit}}$. This value is independent of the junction width and of correlations in the leads. On the contrary, the quasiparticle weight inside the insulating slab is completely borrowed from the leads and strongly depends therefore on their separation and correlation. The quantity which depends strictly on the central slab interaction $U_{\text{center}}>U_{\text{crit}}$ is the quasiparticle decay length ξ_{center} from the lead to the center of the slab, which increases for increasing slab correlation according to the law $(U_{\text{center}}-U_{\text{crit}})^{-\nu}$, with $\nu\approx 0.5$, a value that matches perfectly that found in Sec. I

These results suggest that, if we look at the problem from a transport point of view, we are confronted with two completely different mechanisms. In a strongly correlated metallic central slab, ξ_{center} has the role of a screening length, exactly the same role of ξ_{right} in Sec. II. If instead the central slab is insulating, the meaning of ξ_{center} becomes completely different; it is now a tunneling length. No local quasiparticle peak would survive in a homogeneous Mott insulator: the residual quasiparticle peak that we find inside the central slab is therefore the evanescent lead electron-wave function that

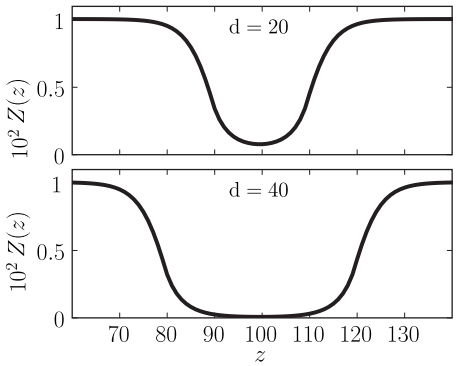

FIG. 12. Same as in Fig. 10, for $U_{\text{left}}=U_{\text{right}}=15.9198t$ and $U_{\text{center}}=16.0288t$.

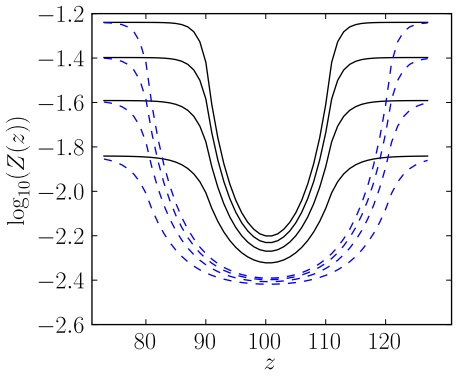

FIG. 13. (Color online) Logarithm of the quasiparticle weight Z as a function of layer index z for a 20-sites-wide (solid line) and 40-sites-wide (dashed line) strongly correlated metallic slab $U=15.9712t<U_{\text{crit}}$ sandwiched between two weakly correlated metal leads (with $U=15.88438t$, $15.79388t$, $15.67674t$, and $15.53236t$). The entire system is 200-sites wide; the interfaces between the leads and the slab are at $z=80$ and $z=120$ for the 40-sites-wide slab and $z=90$ and $z=110$ for the 20-sites-wide slab. The figure shows that for increasing slab width the quasiparticle weight goes to a value that is independent of lead correlation.

tunnels into the slab. In particular, the behavior of Z in the interior of the central slab is well reproduced by the formula (18) that leads to a minimum value[44]

$$Z_{\text{min}} \simeq 64e^{-d/\xi_{\text{center}}}, \tag{23}$$

with ξ_{center} defined in Eq. (20).

A special case is realized when $U_{\text{center}}\approx U_{\text{crit}}$, i.e., right at criticality, where neither of the previous pictures is valid. The transition point between the two opposite exponential decays describing either screening or tunneling is characterized by the absence of any characteristic length, which implies a power-law variation in the quasiparticle strength upon the slab width d

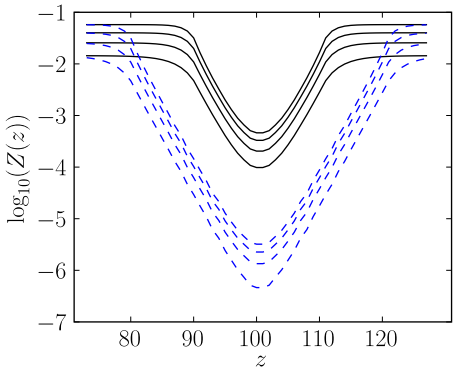

FIG. 14. (Color online) Same as in Fig. 13 but the central layers have now $U=16.1148>U_{\text{crit}}$. In this case the quasiparticle weight at the center of the junction is strongly dependent both on barrier width and on the strength of electron correlation in the leads. The central layer remains metallic for arbitrary values of $U>U_{\text{crit}}$ but its quasiparticle weight decreases exponentially with the slab width.

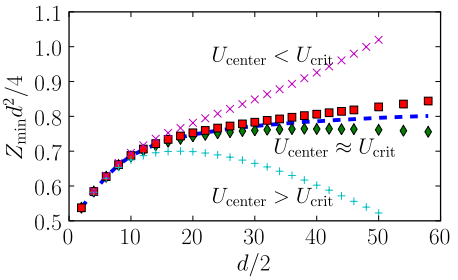

FIG. 15. (Color online) Numerical results for $Z_{min}d^2/4$ and $U=15.999t$ (crosses), $16t$ (squares), $16.0002t$ (dashed line), $16.0004t$ (diamonds), and $16.002t$ (pluses) for the sandwich geometry with $U_{left}=U_{right}=2t$.

$$Z_{min}(d) \sim \frac{3.2}{d^2} + O\left(\frac{1}{d^3}\right) \tag{24}$$

as it emerges from Fig. 15. We find that the leading $1/d^2$ behavior do not, within our accuracy, depend on the specific properties of the metallic leads, and only the subleading terms do, see Fig. 16.

IV. CONCLUSIONS

We presented a study of how the spatial inhomogeneity of interfaces affects the physics of a strongly correlated electron system, over large-distance scales. To address this problem, we extended the conventional Gutzwiller approximation technique to account for inhomogeneous Hamiltonian parameters. In order to cope efficiently with the larger number of variational parameters in comparison with the homogeneous case, we derived iterative equations fully equivalent to the saddle point equations that identify the optimal variational solution, similarly to what is commonly done within unrestricted Hartree-Fock or *ab initio* LDA calculations. These iterative equations can be solved without much effort for very large system sizes. This represents an advantage with respect to more rigorous approaches, such as, e.g., DMFT calculations, which are numerically feasible only for small systems.

We applied the Gutzwiller method to various interface geometries in three dimensions; specifically the interface of a strongly correlated metal with the vacuum, the interface between two differently correlated metals and the junction between two weakly correlated metals sandwiched by a strongly correlated slab. These geometries had been studied by DMFT,[27,28,31–36] with which we can directly compare, providing a test on the quality of our approximation, which is then applicable to much larger sizes.

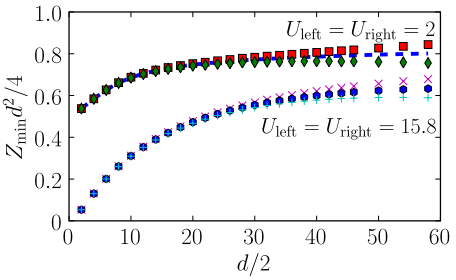

FIG. 16. (Color online) Numerical results for $Z_{min}d^2/4$ for $U_{left}=U_{right}=2t$ [$U_{center}=16t$ (squares), $16.0002t$ (dashed line), and $16.0004t$ (diamonds)], and for $U_{left}=U_{right}=15.8t$ [$U_{center}=16.0002t$ (crosses), $16.0004t$ (hexagons), and $16.0006t$ (pluses)]. The stronger lead correlation in the lower curves pushes the plateau of the function $Z_{min}d^2/4$ toward larger values of d.

Our main result is a clear characterization of the long-distance exponential decay of the metallic character across interfaces. Its dependence on Hamiltonian parameters shows that these interface lengths are in fact correlation lengths that represent bulk properties independent upon the details of the interface and that diverge close to an incipient Mott transition. In particular, at the surface of a strongly correlated metal we find a strong suppression of the metallic properties, e.g., of the quasiparticle weight, that persists on a large depth controlled by the Mott transition correlation length, a dead layer[38] appearing because the surface is effectively more correlated than the bulk and consistent with photoemission experiments.[37] Conversely, metallic features from a metal lead penetrate inside a Mott insulator within a depth that, once again, diverges on approaching the Mott transition. As a consequence, a conducting channel always exists inside a Mott insulating slab contacted to two metallic leads, in agreement with recent DMFT analyses,[35] implying a finite conductance at zero bias and temperature that decays fast on increasing both external parameters on an energy scale exponentially small in the length of the slab in units of the Mott transition correlation length.

The method we develop here being simple and flexible, it can, in principle, be applied to a variety of realistic situations of current interest, not just for interfaces but also for more general inhomogeneities, as those arising by impurities or other defects. With simple generalizations, one can easily incorporate additional features such as magnetism, which we have disregarded throughout this work.

ACKNOWLEDGMENTS

The work was supported by the Italian Ministry of University and Research. The environment provided by the independent ESF project CNR-FANAS-AFRI was also useful.

[1] N. Mott, *Metal Insulator Transition* (Taylor & Francis, London, 1990).
[2] A. Georges, G. Kotliar, W. Krauth, and M. J. Rozenberg, Rev. Mod. Phys. **68**, 13 (1996).
[3] A. Sekiyama, T. Iwasaki, K. Matsuda, Y. Saitoh, Y. Onuki, and S. Suga, Nature (London) **403**, 396 (2000).
[4] K. Maiti, D. D. Sarma, M. J. Rozenberg, I. H. Inoue, H. Makino, O. Goto, M. Pedio, and R. Cimino, Europhys. Lett. **55**, 246 (2001).
[5] S.-K. Mo *et al.*, Phys. Rev. Lett. **93**, 076404 (2004).
[6] A. Sekiyama *et al.*, Phys. Rev. Lett. **93**, 156402 (2004).
[7] N. Kamakura, Y. Takata, T. Tokushima, Y. Harada, A. Chainani, K. Kobayashi, and S. Shin, Europhys. Lett. **67**, 240 (2004).
[8] H.-D. Kim, H.-J. Noh, K. H. Kim, and S.-J. Oh, Phys. Rev. Lett. **93**, 126404 (2004).
[9] M. Taguchi *et al.*, Phys. Rev. B **71**, 155102 (2005).
[10] S.-K. Mo *et al.*, Phys. Rev. B **74**, 165101 (2006).
[11] R. Eguchi *et al.*, Phys. Rev. Lett. **96**, 076402 (2006).
[12] M. Yano *et al.*, Phys. Rev. B **77**, 035118 (2008).
[13] D. B. McWhan and J. P. Remeika, Phys. Rev. B **2**, 3734 (1970).
[14] D. B. McWhan, T. M. Rice, and J. P. Remeika, Phys. Rev. Lett. **23**, 1384 (1969).
[15] W. F. Brinkman and T. M. Rice, Phys. Rev. B **2**, 4302 (1970).
[16] P. D. Dernier and M. Marezio, Phys. Rev. B **2**, 3771 (1970).
[17] G. A. Sawatzky and D. Post, Phys. Rev. B **20**, 1546 (1979).
[18] K. E. Smith and V. E. Henrich, Phys. Rev. B **50**, 1382 (1994).
[19] S. Shin, Y. Tezuka, T. Kinoshita, T. Ishii, T. Kashiwakura, M. Takahashi, and Y. Suda, J. Phys. Soc. Jpn. **64**, 1230 (1995).
[20] R. Zimmermann, R. Claessen, F. Reinert, P. Steiner, and S. Hüfner, J. Phys.: Condens. Matter **10**, 5697 (1998).
[21] G. Panaccione *et al.*, Phys. Rev. Lett. **97**, 116401 (2006).
[22] S.-K. Mo *et al.*, Phys. Rev. Lett. **90**, 186403 (2003).
[23] A. Ohtomo and H. Y. Hwang, Nature (London) **427**, 423 (2004).
[24] N. Reyren *et al.*, Science **317**, 1196 (2007).
[25] See, e.g., Refs. 45–47 and MRS Bull. **33** (2008), for an overview of the status and perspectives of this subject.
[26] R. Pentcheva and W. E. Pickett, Phys. Rev. B **74**, 035112 (2006).
[27] S. Schwieger, M. Potthoff, and W. Nolting, Phys. Rev. B **67**, 165408 (2003).
[28] M. Potthoff and W. Nolting, Phys. Rev. B **60**, 7834 (1999).
[29] S. Okamoto and A. J. Millis, Nature (London) **428**, 630 (2004).
[30] S. Okamoto and A. J. Millis, Phys. Rev. B **70**, 241104(R) (2004).
[31] J. K. Freericks, Phys. Rev. B **70**, 195342 (2004).
[32] A. Liebsch, Phys. Rev. Lett. **90**, 096401 (2003).
[33] L. Chen and J. K. Freericks, Phys. Rev. B **75**, 125114 (2007).
[34] R. W. Helmes, T. A. Costi, and A. Rosch, Phys. Rev. Lett. **101**, 066802 (2008).
[35] H. Zenia, J. K. Freericks, H. R. Krishnamurthy, and T. Pruschke, Phys. Rev. Lett. **103**, 116402 (2009).
[36] H. Ishida, D. Wortmann, and A. Liebsch, Phys. Rev. B **73**, 245421 (2006).
[37] F. Rodolakis *et al.*, Phys. Rev. Lett. **102**, 066805 (2009).
[38] G. Borghi, M. Fabrizio, and E. Tosatti, Phys. Rev. Lett. **102**, 066806 (2009).
[39] M. C. Gutzwiller, Phys. Rev. **134**, A923 (1964).
[40] M. C. Gutzwiller, Phys. Rev. **137**, A1726 (1965).
[41] M. Fabrizio, Phys. Rev. B **76**, 165110 (2007).
[42] J. Bünemann, F. Gebhard, T. Ohm, S. Weiser, and W. Weber, in *Frontiers in Magnetic Materials*, edited by A. Narlikar (Springer, Berlin, 2005), pp. 117–151.
[43] H. J. Monkhorst and J. D. Pack, Phys. Rev. B **13**, 5188 (1976).
[44] See supplementary material at http://link.aps.org/supplemental/10.1103/PhysRevB.81.115134 for approximate analytical expressions of the layer dependence of the quasiparticle weight.
[45] J. Heber, Nature (London) **459**, 28 (2009).
[46] B. Goss Levi, Phys. Today **60**, 23 (2007).
[47] J. W. Reiner, F. J. Walker, and C. H. Ahn, Science **323**, 1018 (2009).